# Microwave Nonlinearities in Anisotropic Dielectrics and Their Relation to Optical and Electro-Optical Nonlinearities

G. D. Boyd and M. A. Pollack
*Bell Telephone Laboratories, Holmdel, New Jersey 07733*
(Received 2 October 1972)

Earlier measurements of the three-frequency microwave nonlinear susceptibility coefficient have been extended to include all of the nonzero tensor components of $d_{ijk}^{m}(-\omega_3,\omega_2,\omega_1)$ of $LiNbO_3$ and $LiTaO_3$. These results are interpreted, using the formalism developed by Lax and Nelson, to describe nonlinearities associated with electronic and ionic modes of anisotropic crystalline materials. The linear dispersion parameters for each material are first approximated by a single-electronic and a single-ionic normal mode. Nonlinear elements are then added to this normal-mode model. A macroscopic-bond-charge model is developed. With some simplifying asumptions and knowledge of the optical nonlinear coefficient $d_{ijk}^{o}$ and the electro-optic coefficient $d_{ijk}^{eo}$, a good fit with the measured values of $d_{ijk}^{m}$ can be obtained. The same parameters used to fit $d_{ijk}^{m}$ are used to calculate the pyroelectric coefficients for $LiNbO_3$ and $LiTaO_3$. In both cases, the correct signs and magnitudes within a factor of 2 of experimental values are obtained.

## I. INTRODUCTION

Nonlinear interactions of three fields, at least two of which are at optical frequencies, have been studied extensively in anisotropic dielectrics. Second-harmonic generation, sum- and difference-frequency generation, the Raman and electro-optic effects, and optical rectification have been observed and well characterized with the help of laser sources for a variety of acentric crystals. Nonlinearities in dielectrics, however, are by no means limited to the optical region. In this paper we deal primarily with nonlinear interactions of three microwave (or radio-frequency) fields,[1] and show how these interactions are related to the better-known phenomena involving optical frequencies.[2]

The application to an anisotropic dielectric of two driving electric fields $E_j(\omega_2)$ and $E_k(\omega_1)$ at frequencies $\omega_2$ and $\omega_1$ gives rise to a nonlinear response at frequency $\omega_3$ which can be described in terms of a generated polarization wave of Fourier amplitude $\mathcal{P}_i(\omega_3)$.[2] The tensor nonlinear susceptibility coefficient $d$ for the mixing of two frequencies is defined in mks units as[3,4]

$$\mathcal{P}_i(\omega_3) = 2\epsilon_0 d_{ijk}(-\omega_3, \omega_2, \omega_1) E_j(\omega_2) E_k(\omega_1) , \tag{1.1}$$

where $\epsilon_0$ is the permittivity of free space. Summation over repeated indices is conventionally implied. The angular frequencies $\omega_3$, $\omega_2$, and $\omega_1$ are arbitrary, except that conservation of energy requires that $\omega_3 = \omega_2 + \omega_1$. For second-harmonic generation, $\omega_2 = \omega_1$ and the factor of 2 is then deleted from Eq. (1.1) to make the definition of $d_{ijk}$ consistent with the definition for mixing.[5]

The magnitude, and often the sign, of a component $d_{ijk}$ of the nonlinear coefficient are known to change markedly as one or more of the frequencies involved is varied from the optical region, through the lattice resonance frequencies, to the microwave region. When $\omega_3$, $\omega_2$, and $\omega_1$ *all* are in the optical region, defined here as the region between the electronic-absorption-band edge and the lattice absorption bands, but not too close to these resonances, the nonlinear coefficient changes little with frequency. We term this optical nonlinear coefficient $d^{o}$, and use it to describe optical mixing or second-harmonic generation.

When the frequency of one of the applied fields is in the microwave region and those of the other applied fields are in the optical region, the electro-optic nonlinear coefficient $d^{eo}$ describes the interaction. The microwave or modulating field is taken to be $E_k(\omega_1)$, which makes the ordering of the subscripts consistent with the usual electro-optic convention. The components of $d^{eo}$ are related to the components of the more common electro-optic coefficient $r$ by[1,5]

$$d_{ijk}^{eo} = -\tfrac{1}{4} n_i^2 n_j^2 r_{ijk} , \tag{1.2}$$

where $n_i$ and $n_j$ are refractive indices (and no summation of subscripts is implied). The electro-optic coefficient also describes optical rectification, in which two optical frequencies are mixed to produce a microwave frequency.

When all three frequencies are in the microwave region, the microwave linear susceptibility coefficient $d^{m}$ describes the mixing process. This coefficient should vary little from frequencies just below the lattice absorption bands, usually corresponding to submillimeter wavelengths, to the low radio frequencies, where piezoelectric effects can no longer be neglected. As long as all frequencies

are kept sufficiently above the acoustic resonance frequencies of the crystal so that piezoelectric contributions to the susceptibility can be ignored, $d^{m}$ and $d^{e\circ}$ will correspond to constant strain or clamped nonlinear coefficients.

Measurements of $d^{m}$ for a large number of polar and nonpolar crystals have recently been reported.[1,6] For each crystal, both the magnitude[1] and sign[6] of one of the tensor components of the clamped coefficient were determined using heterodyne techniques. Other measurements include the determination, using microwave second-harmonic generation, of $|d^{m}_{312}|$ for potassium dihydrogen phosphate (KDP) by Volkova and Yashchin,[7] and the temperature dependence of the same component by Tal'yanskii *et al.*[8] The unclamped coefficient corresponding to $d^{m}_{222}$ has been measured in $LiNbO_3$ by Ivanov and Morozov.[9] A limited number of other measurements on acentric crystals had been reported previously, but insufficient data had been given for a direct comparison with $d^{m}$.[10,11]

It has been observed that values of $d^{m}$ may easily exceed typical values of $d^{\circ}$ by several orders of magnitude for some materials. It was found in particular that materials with large values of linear microwave susceptibility

$$\chi = \chi^{e} + \chi^{i} = \epsilon/\epsilon_0 - 1 \tag{1.3}$$

have extremely large values of $d^{m}$.[1,7-9] In Eq. (1.3),

$$\chi^{e} = n^2 - 1 \tag{1.4}$$

is the electronic linear susceptibility,

$$\chi^{i} = \epsilon/\epsilon_0 - n^2 - 1 \tag{1.5}$$

is the ionic linear susceptibility, and $\epsilon/\epsilon_0$ is the relative dielectric constant.

The connection between large linear susceptibilities and large values of the nonlinear coefficient was first recognized by Miller[12] for $d^{\circ}$. He showed that $d^{\circ}_{ijk}$ could be written empirically as the product of the *linear* susceptibilities at the three frequencies involved and a parameter $\delta$:

$$d^{\circ}_{ijk}(-\omega_3, \omega_2, \omega_1) \equiv \delta^{eee}_{ijk}\chi^{e}_{i}(\omega_3)\chi^{e}_{j}(\omega_2)\chi^{e}_{k}(\omega_1)\ . \tag{1.6}$$

In the optical region, the linear susceptibility is electronic in origin. The frequency dependence of $d^{\circ}$, and to a great extent its variation from material to material, are accounted for by the variations of the linear susceptibilities, leaving $\delta$ a nearly constant parameter. A qualitative explanation of Eq. (1.6) has been found by Garrett and Robinson,[13] based on a classical one-dimensional anharmonic-oscillator model.

When one or more of the frequencies is in the microwave region, ionic as well as electronic contributions to the nonlinear susceptibility are expected. Genkin *et al.*,[14] Garrett,[15] Lax and Nelson,[16] and Flytzanis[17] have treated both ionic and electronic contributions through semiphenomenological theories. Garrett's model is an extension of the one-dimensional anharmonic-oscillator approach to include ionic effects and the coupling between ionic and electronic motion. Four different $\delta$-like parameters multiply combinations of $\chi^{e}$ and $\chi^{i}$ to give $d^{m}$ in this treatment.

In the theory of Lax and Nelson, which also gives the form of the nonlinear coefficient in terms of a number of $\delta$ coefficients, Garrett's work is extended to three dimensions. Lax and Nelson also derive the symmetry conditions that must be obeyed by the $\delta$ coefficients, and verify that $d^{m}$, as well as $d^{\circ}$, must obey over-all permutation (i.e., Kleinman[18]) symmetry conditions when there is no dispersion between the frequencies involved.

The motivation for the present work, which extends earlier measurements[1] to all the nonzero elements of $d^{m}$ for two of the more interesting materials, is the comparison of these experimental results with the prediction of theories based on classical models. Because of their large measured values of $d^{m}_{333}$, the ferroelectric crystals lithium niobate ($LiNbO_3$) and lithium tantalate ($LiTaO_3$) were chosen for further experimental study. Both belong to the $3m$ point group. The nonzero elements of $d^{m}$ are therefore $d^{m}_{333}$, $d^{m}_{222}$, $d^{m}_{311}$, and $d^{m}_{113}$, where the axis 3 coincides with the $c$ axis and the axes 1 and 2 are normal to it. Over-all permutation symmetry requires that $d^{m}_{311}$ and $d^{m}_{113}$ should be equal, as long as dispersion in the linear susceptibilities can be ignored between $\omega_3$, $\omega_2$, and $\omega_1$, which is a reasonable assumption for our experimental conditions.

In Sec. II, we use the results of Lax and Nelson to express $d$ in terms of the coefficients of a general expansion of the anharmonic potential. The nonlinear coefficient is presented as a sum of terms, each a product of a different $\delta$ parameter and three susceptibilities. Expressions are then developed in terms of the $\delta$'s for the particular forms of $d^{\circ}$, $d^{e\circ}$, and $d^{m}$ pertinent to the materials of interest.

The measurements of $d^{m}$ for $LiNbO_3$ and $LiTaO_3$ are reported in Sec. III. Techniques are described for measuring the magnitudes and signs of the four nonzero tensor elements. The results are presented, and compared with the limited data available in the literature.

In Sec. IV we discuss classical normal-mode linear and nonlinear models. By making some simplifying assumptions, the linear parameters for $LiNbO_3$ and $LiTaO_3$ are obtained for a single electronic and a single ionic normal mode. The difficulties involved in treating nonlinearities in the normal-mode frame are also discussed.

A macroscopic-bond-charge model, developed in Sec. V, is used to relate the various $\delta$ coefficients to each other and therefore to enable $d^{m}$ to be predicted from $d^{o}$ and $d^{eo}$. The same model is applied to the pyroelectric effect in Sec. VI.

## II. RELATIONSHIP OF NONLINEAR COEFFICIENT TO LINEAR MATERIAL PARAMETERS AND ANHARMONIC POTENTIAL ENERGY

### A. General Relations

For a collection of oscillators, the terms in the anharmonic potential-energy density which give rise to the nonlinear susceptibility of interest to us are cubic in displacement $y$ from equilibrium[16]:

$$V_a = \sum_{\substack{\lambda\mu\nu \\ ABC}} H^{\lambda\mu\nu}_{ABC}\, y^{\lambda}_{A}\, y^{\mu}_{B}\, y^{\nu}_{C} \ . \tag{2.1}$$

In Eq. (2.1) we have specialized the results of Lax and Nelson[16] to a principle-axis coordinate system ($A$, $B$, $C$) in which all second-rank tensor quantities are diagonal. The superscripts $\lambda$, $\mu$, $\nu$ are summed over the various electronic and ionic normal modes of the system, and the $H$'s are parameters which characterize the material.

In Appendix A it is shown that the nonlinear-susceptibility coefficient can be written in terms of the $H$'s and linear susceptibilities as

$$d_{ijk}(\omega_3, \omega_2, \omega_1) = -\frac{3\epsilon_0^2}{2} \sum_{\lambda\mu\nu} \frac{H^{\lambda\mu\nu}_{ijk}\chi^{\lambda}_{i}(\omega_3)\chi^{\mu}_{j}(\omega_2)\chi^{\nu}_{k}(\omega_1)}{q^{\lambda}q^{\mu}q^{\nu}} \ , \tag{2.2}$$

where $i$, $j$, $k$ are spatial coordinates which are not meant to be summed over. The charge $q^{\lambda}$ and susceptibility $\chi^{\lambda}(\omega)$ are associated with the normal mode $\lambda$. Lax and Nelson[16] have given a more general derivation of Eq. (2.2) valid for nondiagonalized systems, and including the treatment of acoustic modes. The neglect of these additional complications is warranted for the materials and frequency regions of interest here.

The empirical relation between the linear and nonlinear susceptibilities in the optical region, Eq. (1.6), suggests that we define

$$\delta^{\lambda\mu\nu}_{ijk} = -\tfrac{3}{2}\epsilon_0^2 H^{\lambda\mu\nu}_{ijk}/(q^{\lambda}q^{\mu}q^{\nu}) \tag{2.3}$$

so that for any combination of frequencies,

$$d_{ijk}(\omega_3, \omega_2, \omega_1) = \sum_{\lambda\mu\nu} \delta^{\lambda\mu\nu}_{ijk}\chi^{\lambda}_{i}(\omega_3)\chi^{\mu}_{j}(\omega_2)\chi^{\nu}_{k}(\omega_1) \ . \tag{2.4}$$

Again, $i$, $j$, $k$ are coordinates which are not summed. In Ref. 1, some of the terms in Eq. (2.4) were ignored. The neglect of these terms is corrected in Appendix B of this paper.

Although Eq. (2.4) describes the nonlinear susceptibility at any frequency, typical measurements have been made away from resonances. As a simplification we will approximate all of the electronic modes by a single mode ($e$) and all of the ionic modes by a single mode ($i$) for each coordinate direction. Values of $\chi$ for these equivalent modes will be discussed later.

The expressions for $d$ often can be simplified by considering the symmetry properties of $\delta^{\lambda\mu\nu}_{ijk}$. These properties follow from the symmetry properties of $H^{\lambda\mu\nu}_{ijk}$ given in Appendix A. Thus $\delta^{\lambda\mu\nu}_{ijk}$ remains unchanged when the superscripts and subscripts are interchanged in pairs. When the superscripts are all identical we have, for example, $\delta^{eee}_{ijk} = \delta^{eee}_{jki}$, etc. We shall use the notation $\delta^{eee}_{(ijk)}$ to indicate that any permutation of subscripts leaves this coefficient unchanged.

### B. Application to $d_{333}$ and $d_{222}$

The terms in the anharmonic potential which contribute to $d_{333}$ are

$$V_{a333} = H^{eee}_{333}(y^{e}_{3})^3 + 3H^{eei}_{333}(y^{e}_{3})^2 y^{i}_{3} + 3H^{iie}_{333}(y^{i}_{3})^2 y^{e}_{3} + H^{iii}_{333}(y^{i}_{3})^3 \ . \tag{2.5}$$

Starting with a potential of this form but with the notation

$$H^{eee}_{333} = D/V \ , \quad 3H^{eei}_{333} = C/V \ , \quad 3H^{iie}_{333} = B/V \ , \quad H^{iii}_{333} = A/V \ , \tag{2.6}$$

where $V$ is the volume per molecule, that is, the primitive cell, Garrett[15] suggested an expansion equivalent to Eq. (2.2). Using this relation, Akitt *et al.*[19] calculate values of $D$, $C$, and $B$ from the dispersion of electro-optic data.

For three optical frequencies, Eq. (2.4) reduces to

$$d^{o}_{333}(\omega_3, \omega_2, \omega_1) = \delta^{eee}_{333}\chi^{e}_{3}(\omega_3)\chi^{e}_{3}(\omega_2)\chi^{e}_{3}(\omega_1) \ . \tag{2.7}$$

When $\omega_1$ is a microwave frequency, $\chi^{i}_{3}(\omega_1)$ is no longer negligible, and the electro-optic coefficient is given by

$$d^{eo}_{333}(\omega_3, \omega_2, \omega_1) = \delta^{eee}_{333}\chi^{e}_{3}(\omega_3)\chi^{e}_{3}(\omega_2)\chi^{e}_{3}(\omega_1) + \delta^{eei}_{333}\chi^{e}_{3}(\omega_3)\chi^{e}_{3}(\omega_2)\chi^{i}_{3}(\omega_1) \ . \tag{2.8}$$

Note that dispersion of the linear susceptibilities is retained in Eqs. (2.7) and (2.8).

For all three frequencies in the microwave region, none of the ionic terms in Eq. (2.4) can be neglected. For frequencies very low compared with the ionic resonance frequencies (indicated by $\omega \to 0$), *dispersion between* $\omega_3$, $\omega_2$, *and* $\omega_1$ *can be neglected* and we obtain for the microwave mixing coefficient

$$d^{m}_{333} = \delta^{eee}_{333}[\chi^{e}_{3}(0)]^3 + 3\delta^{eei}_{333}[\chi^{e}_{3}(0)]^2\chi^{i}_{3}(0) + 3\delta^{iie}_{333}[\chi^{i}_{3}(0)]^2\chi^{e}_{3}(0) + \delta^{iii}_{333}[\chi^{i}_{3}(0)]^3 \ . \tag{2.9}$$

The above relations for $d_{333}$, Eqs. (2.5)–(2.9), can be applied directly to $d_{222}$ by simply substituting the subscript 2 for 3 where it appears.

### C. Application to $d_{311}$ and $d_{113}$

The terms in the anharmonic potential which contribute to $d_{113}$ and $d_{311}$ are

$$V_{a(311)} = 3H^{eee}_{(311)}\, y^e_3 (y^e_1)^2 + 6H^{eei}_{311}\, y^e_3\, y^e_1\, y^i_1 + 3H^{eei}_{113} (y^e_1)^2 y^i_3 + 6H^{iie}_{311}\, y^i_3\, y^i_1\, y^e_1 + 3H^{iie}_{113} (y^i_1)^2 y^e_3 + 3H^{iii}_{(311)}\, y^i_3 (y^i_1)^2 . \quad (2.10)$$

For three optical frequencies, Eq. (2.4) reduces in this case to

$$d^o_{311}(\omega_3, \omega_2, \omega_1) = \delta^{eee}_{(311)} \chi^e_3(\omega_3) \chi^e_1(\omega_2) \chi^e_1(\omega_1) , \quad (2.11)$$

and

$$d^o_{113}(\omega_3, \omega_2, \omega_1) = \delta^{eee}_{(311)} \chi^e_1(\omega_3) \chi^e_1(\omega_2) \chi^e_3(\omega_1) , \quad (2.12)$$

which are equal in the absence of dispersion in $\chi^e$ between $\omega_3$, $\omega_2$, and $\omega_1$, as was pointed out by Kleinman.[18]

The electro-optic coefficients are given by

$$\begin{aligned} d^{eo}_{311}(\omega_3, \omega_2, \omega_1) &= \delta^{eee}_{311} \chi^e_3(\omega_3) \chi^e_1(\omega_2) \chi^e_1(\omega_1) \\ &\quad + \delta^{eei}_{311} \chi^e_3(\omega_3) \chi^e_1(\omega_2) \chi^i_1(\omega_1) , \\ d^{eo}_{113}(\omega_3, \omega_2, \omega_1) &= \delta^{eee}_{311} \chi^e_1(\omega_3) \chi^e_1(\omega_2) \chi^e_3(\omega_1) \\ &\quad + \delta^{eei}_{113} \chi^e_1(\omega_3) \chi^e_1(\omega_2) \chi^i_3(\omega_1) . \end{aligned} \quad (2.13)$$

These are unequal in general, even if dispersion in $\chi^e$ between $\omega_3$ and $\omega_2$ is neglected.

In the microwave region, all terms are necessary for $d^m_{311}$ and $d^m_{113}$. When dispersion can be neglected in $\chi^i$ and $\chi^e$ between the three frequencies, over-all permutation symmetry is again obeyed and

$$\begin{aligned} d^m_{311} = d^m_{113} &= \delta^{eee}_{(311)} \chi^e_3(0) [\chi^e_1(0)]^2 + 2\delta^{eei}_{311} \chi^e_3(0) \chi^e_1(0) \chi^i_1(0) \\ &\quad + \delta^{eei}_{113} [\chi^e_1(0)]^2 \chi^i_3(0) + 2\delta^{iie}_{311} \chi^i_3(0) \chi^i_1(0) \chi^e_1(0) \\ &\quad + \delta^{iie}_{113} [\chi^i_1(0)]^2 \chi^e_3(0) + \delta^{iii}_{(311)} \chi^i_3(0) [\chi^i_1(0)]^2 , \end{aligned} \quad (2.14)$$

where

$$\delta^{iii}_{311} = \delta^{iii}_{113} = \delta^{iii}_{(311)} . \quad (2.15)$$

## III. MEASUREMENTS OF $d^m_{ijk}$ FOR $LiNbO_3$ AND $LiTaO_3$

### A. Experimental Methods

The four nonzero elements of $d^m$ were measured for $LiNbO_3$ and $LiTaO_3$ using techniques described previously.[1,6] The magnitude of $d^m_{ijk}$ was determined from intensity measurements of sidebands produced when a carrier wave, generated by a millimeter-wave klystron, was mixed with (or modulated by) a radio-frequency modulating field. The carrier frequency $\omega_2/2\pi$ could be varied from 53 to 59 GHz and the modulation frequency $\omega_1/2\pi$ from about 80 to 120 MHz. Thus $\omega_3$, $\omega_2$, and $\omega_1$ are all in the region which lies between the crystal acoustic resonances and the lattice-absorption bands.

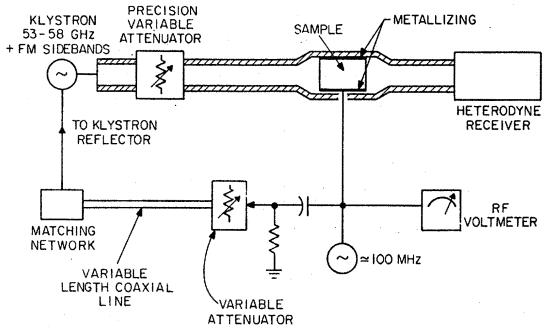


FIG. 1. Experimental arrangement for measuring the ratio $R$ of upper or lower sideband power to carrier power, and the phase of the sidebands relative to the phase of the modulating field.

The crystal samples were mounted in an oversize waveguide section (0.483×0.203 cm) connected to a standard RG-98/U waveguide (0.376 ×0.188 cm) by means of tapered transitions. The millimeter-wave field in the sample was excited by the $TE_{10}$ mode in the waveguide. The only sideband fields that could propagate in the empty waveguide were those in the same mode as the carrier. Because $\omega_1 \ll \omega_2$, $\omega_3$, the dispersion in refractive index between the carrier and sideband waves is unimportant, and phase matching is essentially perfect. Coupling to the output waveguide involves the same loss, reflection, and geometrical factors at both the carrier and sideband frequencies. Therefore, when measuring the ratio $R$ of upper or lower sideband power at $\omega_3$ to carrier power at $\omega_2$, a detailed knowledge of these coupling factors is not required. The power ratio $R$ was measured with the aid of adjustable precision attenuators and a narrowband heterodyne receiver tunable with equal sensitivity to the carrier or sideband frequency. Figure 1 shows schematically the experimental arrangement.

The field at $\omega_1$ was introduced by applying the modulating voltage $V(\omega_1)\cos\omega_1 t$ to silver-paste electrodes on two opposing faces of the crystal through a small hole in the wide wall of the waveguide sample section. The modulating field $E(\omega_1)$, which can be applied either *parallel* to or *perpendicular* to the waveguide fields $E(\omega_2)$ and $E(\omega_3)$, was modeled using an electrostatic resistive sheet analog. These model studies show that in the parallel case, $E(\omega_1)$ is essentially uniform and equal to $V(\omega_1)/b$, where *$b$ is the crystal thickness along $E(\omega_1)$*, whereas in the perpendicular case account must be taken of field distortion (fringing). Averaging over the model field for the crystal-loaded waveguide, the effective modulating field is $FV(\omega_1)/b$. For either $LiNbO_3$ or $LiTaO_3$ in the perpendicu-

lar case, $F \approx 0.88$. In the parallel case, $F = 1$.

When Eq. (1.1) is written in terms of the Fourier amplitudes of the applied microwave fields,

$$\mathcal{P}(\omega_3) = 2\epsilon_0 d^m_{eff} E(\omega_2) E(\omega_1) \ . \qquad (3.1)$$

The effective nonlinear coefficient $d^m_{eff}$ is an element or combination of elements $d^m_{ijk}$ which depends on crystal orientation.

The sideband-to-carrier power ratio for the case of a lossless crystal matched to the waveguide is then[1,20]

$$R = \frac{P(\omega_3)}{P(\omega_2)} \approx \left(\frac{k_3}{\beta_3}\right)^2 \frac{\omega_3^2 (d^m_{eff})^2}{c^2 \epsilon(\omega_3)/\epsilon_0} \left(\frac{l}{b}\right)^2 [V(\omega_1)]^2 F^2 \ , \qquad (3.2)$$

where $l$ is the crystal length and $c$ is the velocity of light. The ratio of the propagation constant for a plane wave in the dielectric to that for the wave in the filled guide, $k_3/\beta_3$, is approximately equal to unity for the cases we consider. The value of the dielectric constant $\epsilon(\omega_3)$ that lies along the waveguide-field direction is used in this expression. As described below, and in Appendix C, Eq. (3.2) must be modified when double refraction is present.

Figure 2 shows the sample geometrics used for the measurements, and gives $d^m_{eff}$ in terms of the tensor components for each case. Crystal samples were typically 1 cm long. The elements $d^m_{333}$ and $d^m_{222}$ were measured directly in the parallel geometry, with crystal heights $b \approx 0.19$ cm and widths about 0.376 cm [Figs. 2(a) and (b)].

To experimentally verify the fringing-field factor $F$, $Fd^m_{112}$ was measured in the perpendicular geometry [Fig. 2(e)]. In this case, $b$, now the width, equals 0.44 cm. The sample height was reduced to about 0.16 cm to keep $F$ near unity. By symmetry, $d^m_{112} \equiv -d^m_{222}$, so that $F$ could be determined. This value of $F$ could then be used to obtain $d^m_{113}$ from a measurement of $Fd^m_{113}$, also in the perpendicular geometry [Fig. 2(d)].

The element $d^m_{311}$ was obtained by measuring the combination coefficient $d^m_c$ for the geometry shown in Fig. 2(c). In this case $d^m_{311} = \sqrt{2}\, d^m_c - \frac{1}{2}(d^m_{113} + d^m_{333})$. Because the fields do not lie either along or normal to the axis 3 of the crystal, account must be taken of double refraction. In Eq. (3.2) replace $\epsilon(\omega_3)$ by $\epsilon(\omega_3, \phi)\cos^2\rho$, where $\phi$ is the angle between the axis 3 and the direction of the Poynting vector, that is, the waveguide axis, and $\rho$ is the double-refraction angle. Appendix C gives expressions for the general case, but for the geometry of Fig. 2(c), $\phi = 45°$ and $\epsilon(\omega_3, \phi)\cos^2\rho = \frac{1}{2}(\epsilon_1 + \epsilon_3)$.

The samples used in our experiments had parallel input and output surfaces, leading to resonant behavior of the sideband and transmitted carrier amplitudes. For the low-loss samples measured, these resonances caused large variations in $R$ as the carrier frequency was varied. An analysis of this effect[21] shows that the value of $R$ that would be obtained in the absence of resonance equals the geometric mean of the experimental power ratios at the resonator transmission maxima and minima. For this reason, values of $R$ were measured as $\omega_2$ was varied from about 53 to 59 GHz to cover several free spectral ranges of the crystal resonance.

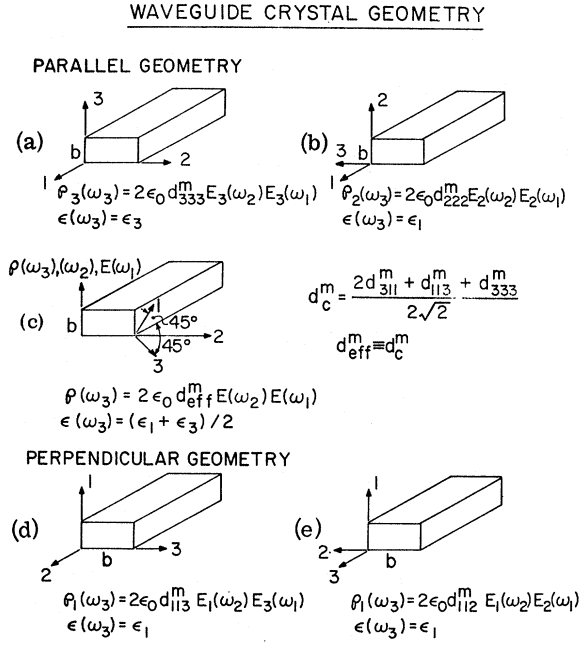


FIG. 2. Sample geometries used to measure the tensor components of $d^m$. Except for case (c), the fields and polarizations lie along principal axes. The effective value of $\epsilon$ depends on the orientation. The modulating field $E(\omega_1)$ is applied across the $b$ dimension.

The signs of the elements of $d^m$ were measured using the technique described by Pollack and Turner.[6] Basically, the sign of $d^m$ determines the phases of the sidebands relative to the phase of the modulating field. The phase of a sideband produced in the crystal through $d^m$ is measured by comparing it with the phase of a frequency-modulation sideband generated by modulating the reflector of the klystron carrier source with a sample of $V_1$. The comparison is made by adjusting the amplitude and phase shift of the sample of $V_1$ coupled to the reflector for cancellation of the sideband components from the two sources. The absolute sign of $d^m$ is then determined from the over-all phase shift.

### B. Experimental Results

The $LiNbO_3$ boule was obtained from Crystal Technology, Inc. Two boules of $LiTaO_3$ were supplied by Ballman of Bell Laboratories. All sam-

TABLE I. Experimental values of $d^m_{eff}$ (in units of $10^{-12}$ m/V). The values of $\epsilon_1$ and $\epsilon_3$ used to reduce the data are from Ref. 22. The fringing-field reduction factor $F$ is obtained from $d^m_{112} \equiv -d^m_{222}$.

| Geometry | $d^m_{eff}$ | $LiNbO_3$ | $LiTaO_3$ |
|---|---|---|---|
| $A$ | $d^m_{333}$ | $-5870 \pm 10\%$ | $-18620 \pm 8\%$ |
| $B$ | $d^m_{222}$ | $-4470 \pm 20\%$ | $-2760 \pm 15\%$ |
| $C$ | $d^m_c$ | $-10760 \pm 3\%$ | $-14740 \pm 10\%$ |
| $D$ | $Fd^m_{113}$ | $-7800 \pm 13\%$ | $-6000 \pm 9\%$ |
| $E$ | $Fd^m_{112}$ | $+3800 \pm 20\%$ | $+2510 \pm 19\%$ |
| | $\epsilon_1$ | 44.3 | 42.6 |
| | $\epsilon_2$ | 27.9 | 42.8 |
| | $F$ | 0.85 | 0.91 |

ples were of single-crystal single-domain material. Two or more samples of each material were prepared for each of the five geometries. Measurements of $R$ were made as a function of $\omega_2$ at least twice for each sample.

Table I gives the values of $d^m_{eff}$ determined experimentally for the five sample geometries. Values of $\epsilon_1$ and $\epsilon_3$ are also given.[22] Typically, a peak-modulating voltage of 282 V, measured with a Hewlett–Packard 410B rf voltmeter, was used for these measurements. The error limits given in the table express the reproducibility of the measurements. The absolute accuracy of $d^m$ was limited by dimensional (~1%), voltmeter (± 5%), and attenuator calibration (± 5%) accuracies.

To obtain the values given in Table I, the results from all runs on a given sample were first averaged. Reproducibility was generally better than ± 15% of this average value. Next, the averages for each sample were combined; it is these averages and their range of reproducibility that appears in the table. Lack of better reproducibility can be ascribed to two factors: (i) excitation of higher-order waveguide modes in the sample, and (ii) non-negligible transmission of carrier around the sample. Experimental efforts to minimize these effects were only partially successful for some of the samples.

Because of the rather large error limits, the differences between the experimental values of the correction factor $F$ for the two materials is not particularly significant. Therefore the average value, 0.88, was used to correct $Fd^m_{113}$ to give $d^m_{113}$. This value is coincidentally equal to the predicted value described above.

The four nonzero elements of $d^m$ are given in Table II, along with the much smaller values of $d^o$ and $d^{eo}$ obtained from the literature.[23,24] The value of $d^m_{311}$ has been extracted from $d^m_c$, $d^m_{333}$, and $d^m_{113}$. We observe that $d^m_{113} = d^m_{311}$ to within the error limits of the original data. As over-all permutation- (i.e., Kleinman) symmetry conditions require this equality, the validity of our experimental technique appears to be established. The average value $\frac{1}{2}(d^m_{113} + d^m_{311}) = d^m_{(311)}$ will be used in the following sections.

The only other reported clamped values of $d^m$ for these materials are those given in Ref. 1 for $|d^m_{333}|$: $6700 \times 10^{-12}$ m/V for $LiNbO_3$ and $16000 \times 10^{-12}$ m/V for $LiTaO_3$. The present results are an improvement over those measurements. A dc measurement of the unclamped $d^m_{222}$ coefficient has also been reported for $LiNbO_3$.[9] After adjustment of that data for the value of $\epsilon_1$ used here, the unclamped value $|d^m_{222}| = 6210 \times 10^{-12}$ m/V is obtained. This is reasonably close to our clamped value of $|d^m_{222}| = 4470 \times 10^{-12}$ m/V given in Table II.

The signs and magnitudes of $d^m_{113}$ for $LiNbO_3$ and $LiTaO_3$ have been predicted by Pollack and Turner.[6] For $LiNbO_3$, they relate the variations of the dielectric constant and the spontaneous polarization with temperature to predict that both $d^m_{333}$ and $d^m_{113}$ are negative and approximately equal in magnitude. From Table II we see that these two components differ by only 18%. The prediction for $LiTaO_3$, based on Jerphagnon's[25] relationship between the $\delta$ coefficients and the spontaneous polarization, is that $d^m_{113} = -8700 \times 10^{-12}$ m/V. This value compares favorably with the experimental value of $-7475 \times 10^{-12}$ m/V given in Table II. Although these simple arguments[6] will not be pursued further here, it is interesting to note how well they predict the relationships between the $d^m_{ijk}$ coefficients.

## IV. CLASSICAL NORMAL-MODE MODELS

In Sec. II, the nonlinear coefficients $d^o$, $d^{eo}$, and $d^m$ were given in terms of equivalent single-

TABLE II. $d_{ijk}$ in units of $10^{-12}$ m/V for $LiNbO_3$ and $LiTaO_3$.

| Material | $ijk$ | $d^o$ [a] | $d^{eo}$ [b] | $d^m$ |
|---|---|---|---|---|
| $LiNbO_3$ | 333 | −40.2 | −181 | −5870 |
| | 222 | +3.15 | −23.5 | −4470 |
| | 311 | | −178 | −7840[c] |
| | 113 | | −59.3 | −8880[d] |
| | (311) | −5.82 | | −8360[e] |
| $LiTaO_3$ | 333 | −19.5 | −171.4 | −18620 |
| | 222 | +2.1 | −2.8 | −2760 |
| | 311 | | −112.6 | −8120[c] |
| | 113 | | −39.2 | −6830[d] |
| | (311) | −1.3 | | −7475[e] |

[a] See Ref. 23.
[b] See Ref. 24 and Eq. (1.2).
[c] Obtained from $d^m_{311} = \sqrt{2}\, d^m_c - \frac{1}{2}(d^m_{113} + d^m_{333})$.
[d] Obtained using $F = 0.88$.
[e] Value taken as $\frac{1}{2}(d^m_{113} + d^m_{311})$.

TABLE III. Normal-mode linear parameters for $LiNbO_3$ and $LiTaO_3$. Masses and charges are normalized to the mass $m_e$ and charge $e$ of a free electron and $V$ is the volume of the primitive cell.

| | $LiNbO_3$ | $LiTaO_3$ |
|---|---|---|
| $\chi_1^e(0)$ | 3.884 | 3.48 |
| $\omega_1^e/2\pi c$ | 54 041 $cm^{-1}$ | 60 252 $cm^{-1}$ |
| $\chi_1^i(0)$ | 39.42 | 38.12 |
| $\omega_1^i/2\pi c$ | 189.8 $cm^{-1}$ | 167.4 $cm^{-1}$ |
| $\chi_3^e(0)$ | 3.544 | 3.50 |
| $\omega_3^e/2\pi c$ | 56 783 $cm^{-1}$ | 60 171 $cm^{-1}$ |
| $\chi_3^i(0)$ | 23.36 | 38.30 |
| $\omega_3^i/2\pi c$ | 287.9 $cm^{-1}$ | 224.7 $cm^{-1}$ |
| $V$ | $53.0\times10^{-30}$ $m^3$ | $52.8\times10^{-30}$ $m^3$ |
| $(m^e/m_e)V$ | 6.74 | 7.46 |
| $(m^i/m_e)V$ | 63 283 | 77 248 |
| $\lvert q^e/e\rvert V$ | 6.74 | 7.46 |
| $\lvert q^i/e\rvert V$ | 7.93 | 8.27 |
| $\lvert q^e/q^i\rvert$ | 0.85 | 0.902 |
| $k_1^e$ | $16.2\times10^{30}$ $N/m^4$ | $21.5\times10^{30}$ $N/m^4$ |
| $k_1^i$ | $1.39\times10^{30}$ $N/m^4$ | $1.33\times10^{30}$ $N/m^4$ |
| $k_3^e$ | $17.9\times10^{30}$ $N/m^4$ | $21.5\times10^{30}$ $N/m^4$ |
| $k_3^i$ | $3.19\times10^{30}$ $N/m^4$ | $2.39\times10^{30}$ $N/m^4$ |

mode linear electronic and ionic susceptibilities and a number of $\delta$ coefficients. Although $\delta^{eee}$ and and $\delta^{eei}$ can be extracted directly from $d^{\circ}$ and $d^{eo}$ [through Eqs. (2.7) and (2.8), for example], the additional measurement of $d^m$ can only yield a combination of $\delta^{iie}$ and $\delta^{iii}$.[1] *A model relating the four $\delta$'s would enable us to either* (a) *separate $\delta^{iie}$ and $\delta^{iii}$ from the measured value of $d^m$ or* (b) *predict $d^m$ from measured values of $d^{\circ}$ and $d^{eo}$*. Because there are four $\delta$ coefficients, such a model must have four nonlinear parameters, unless we can reduce this number by means of physically reasonable assumptions.

### A. Linear Normal-Mode Parameters

First let us consider the equivalent single normal-mode parameters. The classical electronic oscillator is completely described by charge density $q^e$, mass density $m^e$, and spring-constant density $k^e$. The quantities $q^i$, $m^i$, and $k^i$ describe the ionic oscillator. We shall assume that the oscillators along the axes $l=1$, 3 have the same charge and mass densities, and differ only in spring constant.

Each oscillator ($\lambda=e$ or $i$) has a resonant frequency

$$\omega_l^\lambda=(k_l^\lambda/m^\lambda)^{1/2} \tag{4.1}$$

and a linear susceptibility $\chi_l^\lambda(\omega)$ (see Appendix A) which, as $\omega$ approaches zero, becomes

$$\chi_l^\lambda(0)=(q^\lambda)^2/k_l^\lambda\epsilon_0\ . \tag{4.2}$$

The values of $\chi_1^e(0)$, $\omega_1^e$, $\chi_3^e(0)$, and $\omega_3^e$ obtained from a computer least-squares fit of the linear optical-dispersion data for $LiNbO_3$[26] and $LiTaO_3$[27] are given in Table III.

The corresponding ionic parameters are obtained by approximating the ionic linear susceptibility at its low-frequency limit. If $S_j^i$ and $\omega_j^i$ are the strengths and angular frequencies of the $j$th ionic mode,

$$\chi^i=\sum_j \frac{S_j^i}{1-(\omega/\omega_j^i)^2} \tag{4.3}$$

and

$$\chi^i\big|_{\omega\sim0}\approx\sum S_j^i+\sum\frac{S_j^i}{(\omega_j^i)^2}\,\omega^2\ =\chi^i(0)\,[1+(\omega/\omega^i)^2]\ , \tag{4.4}$$

where

$$(\omega^i)^2=\chi^i(0)\Big/\sum\frac{S_j^i}{(\omega_j^i)^2}\ . \tag{4.5}$$

The values of $\chi^i(0)=\epsilon/\epsilon_0-\chi^e(0)-1$ given in Table III were computed from the dielectric constants of Table I. The summations in Eqs. (4.3)–(4.5) were taken over the infrared-active modes measured by Barker *et al.*[28,29] with the addition of a mode at $\omega_j\to\infty$, which is needed to make $\chi^i(0)$ match $\sum S_j^i$ calculated from the infrared data. Values of $\omega^i$ obtained from Eq. (4.5) in this way are given in Table III. Similar results have also been obtained using the mode frequencies and strengths determined by Johnston.[30]

In order to avoid the historical problem of having to determine the three oscillator parameters $q^\lambda$, $m^\lambda$, and $k^\lambda$ from the two measured quantities $\omega^\lambda$ and $\chi^\lambda(0)$, we shall make two simplifying assumptions. The first is that the charge-to-mass ratio for the electronic oscillator, $\lvert q^e/m^e\rvert$, is equal to the ratio for a free electron, $\lvert e/m_e\rvert$. This assumption allows the separation of $\lvert q^e\rvert$, $m^e$, and $k^e$. For the ionic oscillator, we assume that $m^i$ equals the reduced mass of a Nb or Ta ion vibrating against a $LiO_3$ combination, which permits the separation of $\lvert q^i\rvert$, $m^i$, and $k^i$. The use of a reduced mass in the normal-mode frame for the ionic normal-mode mass is justified in Sec. V. The values of these normal-mode linear parameters are given in Table III. The charges given in the table were obtained by averaging the values of $(q_1^\lambda)^2$ and $(q_3^\lambda)^2$ from Eq. (4.2), as we have assumed[16] a single charge for the oscillators along the axes 1 and 3.

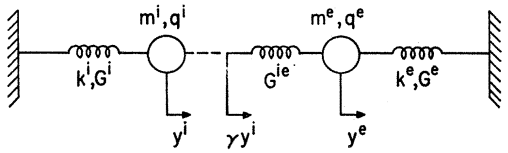


FIG. 3. Normal-mode model of single electronic and single ionic oscillators, including nonlinear springs $G^e$ and $G^i$, and a nonlinear coupling spring $G^{ie}$.

### B. Classical Model of Normal-Mode Nonlinearities

It is difficult to attach a classical meaning to the normal-mode nonlinearities which were introduced in Sec. II through a power series with $H^{\lambda\mu\nu}_{ijk}$ coefficients. A somewhat different approach has been taken by Barker and Loudon,[31] who considered an electronic and an ionic linear oscillator coupled directly by a single nonlinear spring. In our notation, their anharmonic potential energy could be written $G^{ie}(y^i - y^e)^3$. In Fig. 3 we have generalized their model by adding the nonlinear springs $G^i$ and $G^e$ to the ionic and electronic oscillators, and by allowing the nonlinear coupling spring $G^{ie}$ to be compressed by an amount $\gamma y^i - y^e$. The factor $\gamma$ allows for the possibility that the normal-mode displacements $y^i$ and $y^e$ are not equally effective in contributing to a nonlinarity dependent on their relative displacement. The anharmonic part of the potential-energy density which contributes to $d_{333}$, for example, is then

$$V_{a333} = -G^i_{333}(y^i_3)^3 + G^e_{333}(y^e_3)^3 + G^{ie}_{333}(\gamma y^i_3 - y^e_3)^3 . \tag{4.6}$$

When Eq. (4.6) is expanded and compared with Eq. (2.5) one obtains

$$H^{eee}_{333} = G^e_{333} - G^{ie}_{333} , \tag{4.7}$$

$$H^{eei}_{333} = \gamma G^{ie}_{333} , \tag{4.8}$$

$$H^{iie}_{333} = -\gamma^2 G^{ie}_{333} , \tag{4.9}$$

and

$$H^{iii}_{333} = -G^i_{333} + \gamma^3 G^{ie}_{333} . \tag{4.10}$$

This form of $V_{a333}$ is not unique. We have chosen it as a simple extension of the Barker–Loudon model which contains the four required nonlinear parameters and describes the ionic-electronic coupling in a general way.

Barker and Loudon used their model ($G^i = G^e = 0$, $\gamma = \pm 1$) to derive electro-optic coefficients and Raman-scattering cross sections. When the same simplifications are applied to obtain $d^m$ as well, we find from Eqs. (4.7)–(4.10) that all the $H$'s are equal in magnitude. Then $d^m$ always has the same sign as $d^{eo}$, for if we neglect the small dispersion in $\chi^e$ between the optical and microwave frequencies, we can show that

$$d^{eo}/d^o = 1 + C , \tag{4.11}$$

$$d^m/d^o = (1 + C)^3 , \tag{4.12}$$

where

$$C = -\frac{q^e}{q^i}\,\frac{\chi^i(0)}{\chi^e(0)} . \tag{4.13}$$

Although $d^m$ and $d^{eo}$ do have the same signs in $LiNbO_3$ and $LiTaO_3$ (Table II), this is not the case for many other materials (such as GaP and GaAs).[1,6] In addition, $C$, which is the ratio of the ionic to electronic contributions to the electro-optic coefficient,[32] also forces a value of $q^e/q^i$, independent of linear parameters, through the use of this model. The charge ratios calculated in this way depend on the tensor element of $d$, in contrast to our assumption of a common charge for the oscillators along the axes 1 and 3. It is interesting to note that although the Barker–Loudon model cannot meaningfully be extended to predict $d^m_{(311)}$, it does predict values of $d^m_{333}$ only a factor of 2 smaller than the experimental values for $LiNbO_3$ and $LiTaO_3$.

While a single nonlinear parameter cannot properly relate $d^o$, $d^{eo}$, and $d^m$, neither can we obtain four nonlinear parameters from these three pieces of experimental data. It is possible to arbitrarily fix a value of one of the parameters, (such as $\gamma = 1$ or $G^i = 0$) in order to fit the experimental results. Instead, we have found it useful to construct the macroscopic-bond-charge model described in Sec. V. In our opinion, the simplifications and approximations in that model are more physically meaningful than those possible with the normal-mode model. It should be emphasized, however, that the two models are fully equivalent, and it is possible to connect the various coordinates and anharmonic parameters with nonlinear transformation equations [see Eqs. (4.7)–(4.10) and (5.15)–(5.18), and also Ref. 15].

## V. MACROSCOPIC-BOND-CHARGE MODEL

Consider a one-dimensional crystal that consists of a rigid lattice of $a$ ions moving against a rigid lattice of $b$ ions. The two lattices are coupled by appropriate springs, which represent all of the interactions between them. Figure 4 shows the mechanical equivalent circuit representing our one-dimensional system. Between the lattices is a "bond" charge of mass density $m$ and charge density $z$. The ions of mass density $M_a$ and $M_b$ and charge density $Z_a$ and $Z_b$ are coupled to the bond charge by linear springs $k_a$ and $k_b$, and to each other by the linear spring $k_c$. The displacements from equilibrium of the ions and electrons are $u_a$, $u_b$, and $v$. Each spring has a nonlinear part $G$

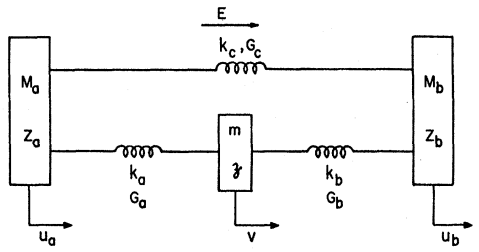


FIG. 4. Mechanical equivalent circuit for the one-dimensional macroscopic-bond-charge model. Rigid-ion lattice "$a$" of mass density $M_a$, charge density $Z_a$, and displacement $u_a$ moves against rigid-ion lattice "$b$." Bond charges of mass density $m$, charge density $z$, and displacement $v$ lie between them. The lattices and bond charge are coupled by linear springs $k$ and nonlinear springs $G$.

which gives rise to the anharmonic terms $V_a$ in the potential energy. Since $G_c$ represents nonlinear coupling between distant ions we shall eventually neglect it.

Our model is a macroscopic one, with the charged lattices acted on directly by the external field $E$, and not by an effective field which includes local-field contributions. The springs describe all the interactions, including Coulomb terms. Johnston,[30] Cowley,[33] Lax and Nelson,[16] and others have pointed out that the inclusion of local-field contributions does not change the form of the potential-energy terms, and that these contributions are all automatically included when the energy expansion parameters are fitted against experiment. Garrett's[15] model, in contrast, is a microscopic model which includes a local-field term. It also differs from ours in that it includes neither a linear spring $k_c$ nor a nonlinear spring $G_c$ between the ion lattices.

### A. Equations of Motions

The kinetic-energy density and the harmonic and anharmonic parts of the potential energy density are given by

$$T = \tfrac{1}{2}M_a(\dot{u}_a)^2 + \tfrac{1}{2}M_b(\dot{u}_b)^2 + \tfrac{1}{2}m(\dot{v})^2 , \tag{5.1}$$

$$V_h = \tfrac{1}{2}k_a(u_a - v)^2 + \tfrac{1}{2}k_b(u_b - v)^2 + \tfrac{1}{2}k_c(u_b - u_a)^2 - (Z_a u_a + Z_b u_b + zv)E , \tag{5.2}$$

and

$$V_a = G_a(u_a - v)^3 + G_b(v - u_b)^2 + G_c(u_a - u_b)^3 . \tag{5.3}$$

The electronic and ionic *normal-mode coordinates* $y^e$ and $y^i$ can be obtained from Eqs. (5.1)–(5.3) by means of the transformation[15]

$$v - u_a = y^e + ry^i , \tag{5.4}$$

$$u_b - u_a = Ay^e + y^i , \tag{5.5}$$

where

$$r = k_b/(k_a + k_b) \tag{5.6}$$

and

$$A = m\left(\frac{(1-r)}{M_a} - \frac{r}{M_b}\right) . \tag{5.7}$$

In terms of the model parameters, the linear normal-mode parameters then are given by

$$q^e = z , \tag{5.8}$$

$$m^e = m , \tag{5.9}$$

$$k^e = k_a + k_b , \tag{5.10}$$

and

$$q^i = (1-r)Z_b - rZ_a , \tag{5.11}$$

$$m^i = M_a M_b/(M_a + M_b) , \tag{5.12}$$

$$k^i = k_c + k_a k_b/(k_a + k_b) . \tag{5.13}$$

Note that a reduced mass is appropriate for the ionic normal mode.

Because $m^e/m^i$ is small compared to 1, $|A| \ll 1$ and the transformed anharmonic potential becomes

$$V_a = -G_a(y^e + ry^i)^3 + G_b[y^e - (1-r)y^i]^3 - G_c(y^i)^3 . \tag{5.14}$$

Our model requires the knowledge of three nonlinear parameters, $G_a$, $G_b$, and $G_c$, as well as the linear parameter $r$. To determine $r$ from Eq. (5.6), we must know $k_a$ and $k_b$. Unfortunately, $k_a$, $k_b$, and $k_c$ cannot be determined separately from knowledge of $k^e$ and $k^i$ through Eqs. (5.10) and (5.13). In the following we will therefore present results using $r$ as an adjustable parameter.

### B. Nonlinear Parameters

When the terms of Eq. (5.14) are rearranged and compared with those of Eq. (2.5) for application to $d_{333}$, we obtain

$$H_{333}^{eee} = -G_{a333} + G_{b333} , \tag{5.15}$$

$$H_{333}^{eei} = -r_3 G_{a333} - (1-r_3)G_{b333} , \tag{5.16}$$

$$H_{333}^{iie} = -r_3^2 G_{a333} + (1-r_3)^2 G_{b333} , \tag{5.17}$$

$$H_{333}^{iii} = -r_3^3 G_{a333} - (1-r_3)^3 G_{b333} - G_{c333} . \tag{5.18}$$

The terms of Eq. (5.14) which contribute to $d_{222}$ give relations of the same form as Eqs. (5.15)–(5.18), but with the subscript 3 replaced by 2 where it appears.

The anharmonic potential $V_a$ described by Eq. (5.14) has been derived from a one-dimensional model. To treat the (311) coefficient, we shall make an *ad hoc assumption* concerning the form of $V_{a(311)}$ as a function of the ionic and electronic displacements along the axes 1 and 3 for a three-dimensional model. From Eq. (2.10) the terms in $V_{a(311)}$ must be products of the form $y_3^\lambda y_1^\mu y_1^\nu$. We choose the simple representation analogous to Eq.

(5.14):

$$V_{a(311)} = -G_{a(311)}(y_3^e + r_3 y_3^i)(y_1^e + r_1 y_1^i)^2 + G_{b(311)}[y_3^e - (1-r_3)y_3^i][y_1^e - (1-r_1)y_1^i]^2 + G_{c(311)} y_3^i (y_1^i)^2 , \quad (5.19)$$

which again requires only three nonlinear springs. Rearranging Eq. (5.19) and comparing with Eq. (2.10), we obtain

$$3H^{eee}_{(311)} = -G_{a(311)} + G_{b(311)} , \quad (5.20)$$

$$3H^{eei}_{311} = -r_1 G_{a(311)} - (1-r_1)G_{b(311)} , \quad (5.21)$$

$$3H^{eei}_{113} = -r_3 G_{a(311)} - (1-r_3)G_{b(311)} , \quad (5.22)$$

$$3H^{iie}_{311} = -r_3 r_1 G_{a(311)} + (1-r_3)(1-r_1)G_{b(311)} , \quad (5.23)$$

$$3H^{iie}_{113} = -r_1^2 G_{a(311)} + (1-r_1)^2 G_{b(311)} , \quad (5.24)$$

$$3H^{iii}_{(311)} = -r_3 r_1^2 G_{a(311)} - (1-r_3) \times (1-r_1)^2 G_{b(311)} - G_{c(311)} . \quad (5.25)$$

*It should be noted that Eq.* (5.19) *is by no means a unique description of the anharmonic potential in three dimensions.* However, a more general form would involve more parameters than could be evaluated from experimental data.

### C. Comparison of the Bond-Charge Theory with Experiment

Up to this point, only absolute values of the charges $q^e$ and $q^i$ have been determined. We now arbitrarily choose both of these quantities to be negative. Determination of $d^m$ requires the ratio $q^e/q^i$, which we have taken as positive. With this choice of sign, the bond charge $z = q^e$ is negative. Had we chosen the reverse sign for $q^i$, the results would be unchanged, except for an interchange of $r$ and $(1-r)$, and $Z_a$ and $Z_b$, according to Eq. (5.11).

As described in Sec. V A, we will treat $r_1$ and $r_3$ as adjustable parameters when comparing the values of $d^m$ predicted using the bond-charge model with those obtained experimentally. First, $\delta^{eee}$ and $\delta^{eei}$ are calculated from $d^o$ and $d^{eo}$ (Table II) and the linear susceptibilities (Table III). Together with $q^e$ and $q^i$ (Table III), this permits the evaluation of $H^{eee}$ and $H^{eei}$ from Eq. (2.3) and then $G_a$ and $G_b$ from Eqs. (5.15) and (5.16), or (5.20) and either of (5.21) or (5.22). Use of the $d^{eo}_{311}$ data and Eq. (5.21) will generally give different values of $G_{a(311)}$ and $G_{b(311)}$ than will $d^{eo}_{113}$ and Eq. (5.22). This difference is a measure of the approximation in using Eq. (5.19) to describe $V_{a(311)}$. The *average* of $G_{a(311)}$ and $G_{b(311)}$ from the two sets of data was used to obtain $d^m_{(311)}$. Results using $d^{eo}_{311}$ or $d^{eo}_{113}$ data separately generally differed from this value by no more than 50%.

The nonlinear spring $G_c$ represents direct coupling between the distant ions. We shall make the *approximation* that this nonlinear coupling is small, and set $G_c = 0$. It is possible, of course, to transform from the macroscopic bond-charge parameters to the normal-mode nonlinear parameters of Sec. IV B. However, no single parameter in the normal-mode model has as simple a physical significance as $G_c$. It is the more physical interpretation of the parameters that makes the macroscopic-bond-charge model the more useful one to us.

Observe in Eqs. (5.18) and (5.25) that $G_c$ contributes only to $H^{iii}$ and not to $H^{iie}$. We can now evaluate $H^{iie}$ and $H^{iii}$ using the relations of Sec. V B, and then evaluate $\delta^{iie}$ and $\delta^{iii}$ using Eq. (2.3). Finally, $d^m$ can be calculated from the relations of Sec. II.

TABLE IV. Comparison of experimental values and the range of calculated values of $d^m_{ijk}$ (in units of $10^{-12}$ m/V). The last column is the result for $r_1 = r_3 = 1$. The second column from the right was obtained using values of $r_1$ and $r_3$ which give the greatest disagreement with experiment.

| Material | $ijk$ | $d^m$ (expt) | $d^m$ (calc) |
|---|---|---|---|
| $LiNbO_3$ | 333 | −5870 | −1094 → −6352 |
| | 222 | −4470 | −329 → −2289 |
| | (311) | −8360 | +400 → −7620 |
| $LiTaO_3$ | 333 | −18620 | −3263 → −17100 |
| | 222 | −2760 | +60 → −551 |
| | (311) | −7475 | +358 → −8456 |

Table IV is a comparison of the experimental values of $d^m$ and the range of calculated values as $r_1$ and $r_3$ are allowed to vary between their limits of 0 and 1. For $d^m_{333}$ and $d^m_{222}$, the poorest agreement occurs for $r_3$ or $r_1$ midway between the limits, while for $d^m_{(311)}$ the poorest agreement is for $r_1 = 0$ and $r_3 = 1$. The best agreement in general occurs for $r_1 \approx r_3 \approx 1$. It is interesting to note that $r = 1$ in the macroscopic-bond-charge model corresponds to $\gamma = -1$ in the normal-mode model of Sec. IV B. Values of $d^m$ calculated for $r_1 = r_3 = 1$ are shown in the last column of the table. Agreement is excellent for $d^m_{333}$ and $d^m_{(311)}$, while it is poorest for $d^m_{222}$, especially in $LiTaO_3$.

Note that whatever the values of $r_1$ or $r_3$, that is, no matter how the linear springs are distributed, this model gives order-of-magnitude agreement with experiment. Perfect agreement with experiment can always be obtained by choosing not to assume that $G_c = 0$.

*We have shown, however, that a model with only two nonlinear elements can reasonably describe* $d^o$, $d^{eo}$, *and* $d^m$ *if one assumes that the bond charge is linearly coupled to a single lattice* ($r_1 = r_3 = 1$) *but nonlinearly coupled to both lattices.*

In Table V are given the values of $\delta^{iie}$ and $\delta^{iii}$

TABLE V. $\delta_{ijk}$ in units of $10^{-12}$ m/V for $LiNbO_3$ and $LiTaO_3$.

| Material | $ijk$ | $\delta^{eee}$ [a] | $\delta^{eei}$ [a] | $\delta^{iie}$ [b] | $\delta^{iii}$ [b] |
|---|---|---|---|---|---|
| $LiNbO_3$ | 333 | −0.761 | −0.421 | −0.358 | −0.304 |
| | 222 | +0.0444 | −0.0373 | −0.0317 | −0.0269 |
| | 311 | −0.0914 | −0.267 | −0.167 | −0.142 |
| | 113 | −0.0914 | −0.127 | −0.167 | −0.142 |
| $LiTaO_3$ | 333 | −0.393 | −0.280 | −0.253 | −0.228 |
| | 222 | +0.043 | −0.0092 | −0.0083 | −0.0075 |
| | 311 | −0.026 | −0.208 | −0.126 | −0.113 |
| | 113 | −0.026 | −0.0707 | −0.126 | −0.113 |

[a]Obtained from experimental values of $d^o$ and $d^{eo}$.
[b]Computed from model using $r_1 = r_3 = 1$.

calculated for $r_1 = r_3 = 1$, as well as the experimental values of $\delta^{eee}$ and $\delta^{eei}$ obtained from $d^o$ and $d^{eo}$. Except for $\delta^{eee}_{222}$, all the $\delta$'s are negative. For each coefficient, the four $\delta$'s are generally comparable in magnitude.

## VI. APPLICATIONS OF MODEL AND CONCLUSIONS

### A. Pyroelectric Effect

Garrett[15] has pointed out that one-dimensional crystal models which possess a polar axis and lack a center of symmetry should allow the prediction of the pyroelectric coefficient. This notion has been pursued by Soref.[34]

Consider the single electronic and ionic modes in the polar (3-axis) direction. In the absence of a driving field, the sum of the harmonic and anharmonic potential-energy densities is given, from Eqs. (2.5) and (A2) as

$$V_{333} = \tfrac{1}{2} k_3^e (y_3^e)^2 + \tfrac{1}{2} k_3^i (y_3^i)^2 + V_{a333} \,. \tag{6.1}$$

The minimum in potential energy is obtained by setting $\partial V_{333}/\partial y_3^e = 0 = \partial V_{333}/\partial y_3^i$. Following Garrett, if we assume $kT \approx \hbar\omega^i \ll \hbar\omega^e$, then the average electronic and ionic displacements are given by

$$k^e \langle y_3^e \rangle = -3H^{iie}_{333} \langle (y_3^i)^2 \rangle \tag{6.2}$$

and

$$k^i \langle y_3^i \rangle = -3H^{iii}_{333} \langle (y_3^i)^2 \rangle \,. \tag{6.3}$$

The average thermal energy per unit volume is related to the heat capacity per unit volume by

$$C_v = \frac{d}{dT}\left(\frac{k_3^i}{2} \langle (y_3^i)^2 \rangle\right). \tag{6.4}$$

The pyroelectric coefficient, defined as

$$p = \frac{d(q^e \langle y_3^e \rangle + q^i \langle y_3^i \rangle)}{dT} \,, \tag{6.5}$$

can then be written as

$$p = \frac{4C_v q^i}{(k_3^i)^2}\left[\left(\frac{k_3^i}{k_3^e}\right)\left(\frac{q^e}{q_i}\right) H^{iie}_{333} + H^{iii}_{333}\right] \,. \tag{6.6}$$

Combining Eq. (6.6) with Eqs. (2.3) and (4.2), we obtain

$$p = 4C_v[\chi_3^i(0)]^2\left(\frac{\chi_3^e(0)}{\chi_3^i(0)}\,\delta^{iie}_{333} + \delta^{iii}_{333}\right) \,. \tag{6.7}$$

The heat capacity of the single ionic normal mode in the primitive cell of volume $V$ (see Table III) will be assumed to be given by

$$VC_v = k_B \theta^2 e^\theta/(e^\theta - 1)^2 \,, \tag{6.8}$$

where $k_B$ is Boltzmann's constant and $\theta = \omega_3^i/k_B T$.

Table VI lists the values of the pyroelectric coefficient calculated using the values of $\delta^{iie}_{333}$ and $\delta^{iii}_{333}$ from Table V, along with measured values taken from the literature.[35,36] The negative sign of $p$ is predicted for both materials, and the measured and calculated magnitudes agree within a factor of about 2 for $LiNbO_3$ and $LiTaO_3$.

### B. Other Applications of Model

The bond-charge model developed in Sec. V allows only for $k = 0$ optical phonons. It does not include the possibility of acoustic phonons. However, if we assume that the same linear spring constants and nonlinearities are involved in acoustic modes as in optical modes, then the thermal-expansion coefficient may be estimated.[37,38] This connection to the thermal-expansion coefficient has been discussed by Kleinman[37] for the case of GaP. Kleinman also discusses the relation of lattice anharmonicities to the strength and temperature shift of the infrared combination bands.

Another possible application of these model parameters is to the calculation of the variation of $d^o$ in spontaneous parametric emission experiments[39–41] in $LiNbO_3$ as the lower frequency decreases and moves into the lattice absorption region. Inclusion of the term $\delta^{eei}$ and perhaps even $\delta^{iie}$ and $\delta^{iii}$ then becomes necessary. Under such circumstances loss must be included in the linear ionic-susceptibility representation.

### C. Conclusions

The measurements we have presented completely specify the microwave nonlinear susceptibility tensor $d^m_{ijk}$ for $LiNbO_3$ and $LiTaO_3$. Values of $d^m$ are

TABLE VI. Comparison of calculated and experimental values of the pyroelectric coefficient for $LiNbO_3$ and $LiTaO_3$. $C_v$ is in units of $J/m^3\,°K$. $p$ is in units of $C/m^2\,°K$.

| | $LiNbO_3$ | $LiTaO_3$ |
|---|---|---|
| $C_v$ | $0.221 \times 10^6$ | $0.236 \times 10^6$ |
| $p$ (expt) | $-0.83 \times 10^{-4}$ [a] | $-1.9 \times 10^{-4}$ [b] |
| $p$ (calc) | $-1.73 \times 10^{-4}$ | $-3.48 \times 10^{-4}$ |

[a]See Ref. 35. [b]See Ref. 36.

much larger than the corresponding values of $d^{\circ}$ and $d^{e\circ}$. The differences can be explained satisfactorily by differences in linear susceptibilities at the various frequencies, for it has been shown that the $\delta$ coefficients are comparable for electronic and ionic contributions to $d$.

The nonlinear coefficients have been written in terms of the parameters of both a normal-mode model and a macroscopic-bond-charge model. By assuming $G_c = 0$ in the latter model, a good fit has been obtained with measured values of $d^m$ for $r_1 \approx r_3 \approx 1$. In the limit of $r_1 = r_3 = 1$, the bond charge is linearly coupled to a single lattice, but nonlinearly to both lattices. Transformation to the normal-mode model for this case shows that $G^i = 0$ and $\gamma = -1$, but this could not be assumed initially. It was the somewhat more physical picture of the macroscopic-bond-charge model that led to the assumption $G_c = 0$.

The nonlinear parameters $\delta_{333}^{iie}$ and $\delta_{333}^{iii}$ obtained with $r_1 = r_3 = 1$ have also been used to predict the pyroelectric coefficients for $LiNbO_3$ and $LiTaO_3$. Agreement with measured values in both cases is within a factor of 2, further demonstrating the utility of the macroscopic-bond-charge model.

The microwave nonlinear susceptibility coefficient $d_{ijk}^m$ discussed in this and previous papers is in our view a fundamental macroscopic parameter of acentric materials and deserving of further study.


## ACKNOWLEDGMENTS

The authors have benefited greatly from the help of many of their colleagues in this work. D. A. Kleinman, M. Lax, and D. F. Nelson have been especially helpful in clarifying many aspects of the theory and its interpretation. The authors are indebted to J. P. Gordon, J. M. Worlock, E. H. Turner, J. F. Scott, W. D. Johnston, and C. K. N. Patel for many stimulating discussions and for their critical comments and help with the manuscript.


## APPENDIX A: DERIVATION OF $d_{ijk}$ FROM THE ANHARMONIC POTENTIAL ENERGY

In this appendix we develop the form of the nonlinear-susceptibility coefficient $d_{ijk}(\omega_3, \omega_2, \omega_1)$ of a material in terms of its linear properties and the expansion coefficients of the anharmonic terms in the potential energy. Consider a system of electrons and ions in a center-of-mass frame. Let $y_A^{\alpha}$, $y_B^{\beta}$, and $y_C^{\gamma}$ be a set of normal-mode displacements from equilibrium which we assume to be along the principle-axis coordinates $A$, $B$, and $C$. The superscripts $\alpha$, $\beta$, $\gamma$ stand for either electronic ($e$) or ionic ($i$) quantities. Associated with the electron lattice is a volume charge density $q^e$ and mass density $m^e$, and with the ion lattice a volume charge density of $q^i$ and mass density $m^i$.

The kinetic-energy density associated with a particular mode $\lambda$ (either electronic or ionic) is

$$T = \tfrac{1}{2} m^{\lambda} [(\dot{y}_A^{\lambda})^2 + (\dot{y}_B^{\lambda})^2 + (\dot{y}_C^{\lambda})^2] \,. \tag{A1}$$

The potential-energy density $V$ is the sum of the harmonic part $V_h$ and the anharmonic part $V_a$, where

$$V_h = \tfrac{1}{2}[k_A^{\lambda}(y_A^{\lambda})^2 + k_B^{\lambda}(y_B^{\lambda})^2 + k_C^{\lambda}(y_C^{\lambda})^2] - q^{\lambda}(E_A y_A^{\lambda} + E_B y_B^{\lambda} + E_C y_C^{\lambda}) \,. \tag{A2}$$

The applied macroscopic electric field with components $E_A$, $E_B$, and $E_C$ supplies the driving force for the system, and the restoring forces are measured by the linear spring constants per unit volume $k_A^{\lambda}$, $k_B^{\lambda}$, and $k_C^{\lambda}$.

Let us examine a displacement $y_l^{\lambda}$ along a particular coordinate $l$. The Lagrangian equation of motion is

$$\frac{d}{dt}\left(\frac{\partial \mathcal{L}}{\partial \dot{y}_l^{\lambda}}\right) - \frac{\partial \mathcal{L}}{\partial y_l^{\lambda}} = 0 \,, \tag{A3}$$

where

$$\mathcal{L} = T - (V_h + V_a) \,. \tag{A4}$$

Substituting for $T$ and $V_h$ from Eqs. (A1) and (A2) into Eq. (A3),

$$\ddot{y}_l^{\lambda} + (\omega_l^{\lambda})^2 y_l^{\lambda} = \frac{q^{\lambda}}{m^{\lambda}} E_l - \frac{1}{m^{\lambda}} \frac{\partial V_a}{\partial y_l^{\lambda}} \,, \tag{A5}$$

where

$$\omega_l^{\lambda} = (k_l^{\lambda}/m^{\lambda})^{1/2} \tag{A6}$$

is the resonant frequency of the electron or ion mode along the $l$ axis. We consider first the linear properties of the system by setting $V_a = 0$ in Eq. (A5). Now an applied field $E_l = \hat{E}_l \cos\omega t$ produces a displacement $y_l^{\lambda} = \hat{y}_l^{\lambda} \cos\omega t$. Then, from Eq. (A5),

$$\hat{y}_l^{\lambda}(\omega) = \frac{q^{\lambda}}{m^{\lambda}} \frac{\hat{E}_l(\omega)}{[(\omega_l^{\lambda})^2 - \omega^2]} \,. \tag{A7}$$

The peak polarization density

$$\hat{P}_l^{\lambda}(\omega) = q^{\lambda} \hat{y}_l^{\lambda}(\omega) = \hat{E}_l(\omega) \chi_l^{\lambda}(\omega) \,, \tag{A8}$$

so that

$$\hat{y}_l^{\lambda}(\omega) = \epsilon_0 \hat{E}_l \chi_l^{\lambda}(\omega)/q^{\lambda} \,, \tag{A9}$$

where

$$\chi_l^{\lambda}(\omega) = \frac{(q^{\lambda})^2/m^{\lambda}\epsilon_0}{[(\omega_l^{\lambda})^2 - \omega^2]} \tag{A10}$$

is the partial linear susceptibility.

The nonlinear excitation at $\omega_3$ due to driving fields at $\omega_1$ and $\omega_2$ can now be written, from Eq. (A5), as

$$\hat{y}_i^\lambda(\omega_3)\cos\omega_3 t = \frac{-1}{m^\lambda[(\omega_i^\lambda)^2-\omega_3^2]}\frac{\partial V_a}{\partial y_i^\lambda} = \frac{-\epsilon_0\chi_i^\lambda(\omega_3)}{(q^\lambda)^2}\frac{\partial V_a}{\partial y_i^\lambda} \quad . \tag{A11}$$

The most general form of the anharmonic potential, following Lax and Nelson,[16] is

$$V_a = \sum_{\substack{ABC\\ \alpha\beta\gamma}} H_{ABC}^{\alpha\beta\gamma}\, y_A^\alpha\, y_B^\beta\, y_C^\gamma \ . \tag{A12}$$

Because the subscripts and superscripts on the expansion coefficients $H_{ABC}^{\alpha\beta\gamma}$ are arbitrary, it is clear that the symmetry of $H$ is such that it remains unchanged on simultaneous interchange of pairs of them. Thus $H_{ABC}^{\alpha\beta\gamma} = H_{BAC}^{\beta\alpha\gamma} = H_{CBA}^{\gamma\beta\alpha}$, etc. There are three different kinds of terms in the sum (A12). In case 1, each of the $y$'s is different, either because of different superscripts or subscripts, or both. In case 2, two of the $y$'s are identical; and in case 3, all three are identical.

Consider the contributions of the case 1 terms to Eq. (A11). Permitting $\alpha$, $\beta$, and $\gamma$ to each take on the specific values $\lambda$, $\mu$, and $\nu$, and $A$, $B$, and $C$ to each take on the values $l$, $m$, and $n$, we obtain the terms of the form

$$H_{lmn}^{\lambda\mu\nu}\, y_l^\lambda\, y_m^\mu\, y_n^\nu + H_{mln}^{\mu\lambda\nu}\, y_m^\mu\, y_l^\lambda\, y_n^\nu + \cdots \ .$$

There are six of these permutations, all equal by the symmetry of $H$, so that the contribution of case 1 terms is $6\sum_{\lambda\mu\nu} H_{lmn}^{\lambda\mu\nu}\, y_l^\lambda\, y_m^\mu\, y_n^\nu$. Note that there is no summation over the subscripts. Then

$$\frac{\partial V_a}{\partial y_l^\lambda} = 6\sum_{\mu\nu} H_{lmn}^{\lambda\mu\nu}\, y_m^\mu\, y_n^\nu \ . \tag{A13}$$

Writing $y_m^\mu = \hat{y}_m^\mu(\omega_2)\cos\omega_2 t$ and $y_n^\nu = \hat{y}_n^\nu(\omega_1)\cos\omega_1 t$, the component of Eq. (A13) at $\omega_3 = \omega_2 + \omega_1$ is

$$\left.\frac{\partial V_a}{\partial y_l^\lambda}\right|_{\omega_3} = 3\sum_{\mu\nu} H_{lmn}^{\lambda\mu\nu}\,\hat{y}_m^\mu(\omega_2)\hat{y}_n^\nu(\omega_1)\cos\omega_3 t \ . \tag{A14}$$

Now consider the three equal case 2 terms which give a contribution $3H_{lnn}^{\lambda\nu\nu}\, y_l^\lambda (y_n^\nu)^2$ to $V_a$. Letting $y_n^\nu = \hat{y}_n^\nu(\omega_1)\cos\omega_1 t + \hat{y}_n^\nu(\omega_2)\cos\omega_2 t$,

$$\left.\frac{\partial V_a}{\partial y_l^\lambda}\right|_{\omega_3} = 3\sum_{\nu} H_{lnn}^{\lambda\nu\nu}\,\hat{y}_n^\nu(\omega_2)\hat{y}_n^\nu(\omega_1)\cos\omega_3 t \ . \tag{A15}$$

Letting $y_l^\lambda = \hat{y}_l^\lambda(\omega_2)\cos\omega_2 t$ and $y_n^\nu = \hat{y}_n^\nu(\omega_1)\cos\omega_1 t$, the terms $3H_{lln}^{\lambda\lambda\nu}(y_l^\lambda)^2 y_n^\nu$ give

$$\left.\frac{\partial V_a}{\partial y_l^\lambda}\right|_{\omega_3} = 3\sum_{\lambda\nu} H_{lln}^{\lambda\lambda\nu}\,\hat{y}_l^\lambda(\omega_2)\hat{y}_n^\nu(\omega_1)\cos\omega_3 t \ . \tag{A16}$$

Finally we treat case 3, which contributes a term $H_{lll}^{\lambda\lambda\lambda}(y_l^\lambda)^3$ to $V_a$. Letting $y_l^\lambda = \hat{y}_l^\lambda(\omega_2)\cos\omega_2 t + \hat{y}_l^\lambda(\omega_1)\cos\omega_1 t$,

$$\left.\frac{\partial V_a}{\partial y_l^\lambda}\right|_{\omega_3} = 3H_{lll}^{\lambda\lambda\lambda}\,\hat{y}_l^\lambda(\omega_2)\hat{y}_l^\lambda(\omega_1)\cos\omega_3 t \ . \tag{A17}$$

*The three cases all give the same resulting form*, so that we can write for the general case of any $l$, $m$, $n$,

$$\left.\frac{\partial V_a}{\partial y_l^\lambda}\right|_{\omega_3} = 3\sum_{\mu\nu} H_{lmn}^{\lambda\mu\nu}\,\hat{y}_m^\mu(\omega_2)\hat{y}_n^\nu(\omega_1)\cos\omega_3 t \ . \tag{A18}$$

Substituting into Eq. (A11), and making use of Eq. (A9),

$$\hat{y}_l^\lambda(\omega_3) = \frac{-3\epsilon_0^3\chi_l^\lambda(\omega_3)}{(q^\lambda)^2}\sum_{\mu\nu}\frac{H_{lmn}^{\lambda\mu\nu}\chi_m^\mu(\omega_2)\chi_n^\nu(\omega_1)}{q^\mu q^\nu}\hat{E}_m\hat{E}_n \ . \tag{A19}$$

From Eq. (1.1), the nonlinear polarization

$$\hat{\mathcal{P}}_i = 2\epsilon_0 d_{ijk}(\omega_3,\omega_2,\omega_1)\hat{E}_j\hat{E}_k = \sum_\lambda q^\lambda\hat{y}(\omega_3) \ . \tag{A20}$$

Substituting Eq. (A19) into Eq. (A20),

$$d_{ijk}(\omega_3,\omega_2,\omega_1) = \frac{-3\epsilon_0^2}{2}\sum_{\lambda\mu\nu}\frac{H_{ijk}^{\lambda\mu\nu}\chi_i^\lambda(\omega_3)\chi_j^\mu(\omega_2)\chi_k^\nu(\omega_3)}{q^\lambda q^\mu q^\nu} \ . \tag{A21}$$

## APPENDIX B

In Ref. 1 the distinguishable frequency permutations illustrated in Eq. (2.7) were ignored. Consequently, Eqs. (3) and (4) of Ref. 1 must be revised as follows. In the notation of that paper, Eq. (3) for the general one-dimensional mixing coefficient should be

$$d(-\omega_3,\omega_2,\omega_1) = \delta_A\chi_1^i\chi_2^i\chi_3^i + \delta_B(\chi_1^i\chi_2^i\chi_3^e + \chi_1^i\chi_2^e\chi_3^i + \chi_1^e\chi_2^i\chi_3^i) + \delta_C(\chi_1^i\chi_2^e\chi_3^e + \chi_1^e\chi_2^i\chi_3^e + \chi_1^e\chi_2^e\chi_3^i) + \delta_D\chi_1^e\chi_2^e\chi_3^e \ . \tag{B1}$$

Similarly, Eq. (4), which neglects dispersion, becomes

$$d^\circ = (\chi^e)^3\delta_D \ ,$$

TABLE VII. Revision of Table I of Ref. 1, corrected according to Eq. (B1). The signs of $d^m$ are taken from Ref. 6.

| Material | $d^m$ | $\delta_{AB}$ | Measured $d_{ijk}$ |
|---|---|---|---|
| $BaTiO_3$ | −97 000 | −0.55 | 333 |
| $LiTaO_3$ | −18 620[a] | −0.25 | 333 |
| $LiNbO_3$ | −5870[a] | −0.29 | 333 |
| $KH_2PO_4$ | −1850 | −0.03 | 123 |
| $NH_4H_2PO_4$ | −970 | −0.007 | 123 |
| $LiIO_3$ | −177 | −1.7 | 333 |
| $NaNO_2$ | 36 | ±1.4 | 333 |
| ZnO | −176 | −0.5 | 333 |
| CdS | −127 | −0.5 | 333 |
| CdTe | ±36 | Ref. b | 123 |
| GaP | −24 | Ref. b | 123 |
| GaAs | −51 | Ref. b | 123 |
| $Ag_3AsS_3$ | ±950 | ~±0.1 | 333 |

[a]Revised values from this paper.

[b]The closeness in values of $d^m$, $d^{eo}$, $d^\circ$ and their uncertainties prevents a meaningful calculation of $\delta_{AB}$ in this approximation of no dispersion.

$$d^{eo} - d^{o} = \chi^{i}(\chi^{e})^{2}\delta_{C} ,$$

$$d^{m} = d^{o} - 3(d^{eo} - d^{o}) = (\chi^{i})^{2}(\chi^{i}\delta_{A} + 3\chi^{e}\delta_{B})$$

$$\equiv (\chi^{i})^{2}(\chi^{i} + 3\chi^{e})\delta_{AB} , \qquad \text{(B2)}$$

where $\delta_{AB}$ is a defined parameter which equals $\delta_A$ if $\delta_A = \delta_B$.

A revision of Table I of Ref. 1 for the appropriate columns is given in Table VII. The signs for $d^m$ are taken from Pollack and Turner.[6] It is interesting to note that for $LiNbO_3$ and $LiTaO_3$, $\delta_D$, $\delta_C$, and $\delta_{AB}$ are all nearly equal.

## APPENDIX C: DOUBLE REFRACTION

Double refraction must be considered when the waveguide field is polarized as an extraordinary wave (the electric field lies in the plane containing the optic or 3 axis and the direction of propagation). This is the case for the geometries shown in Figs. 2(a), (c), and (e). Then in Eq. (3.2), $\epsilon(\omega_3)$ must be replaced by $\epsilon(\omega_3, \phi)\cos^2\rho$, where $\phi$ is the angle between the Poynting vector direction (the waveguide axis) and the 3 axis. The double-refraction angle $\rho$ is measured between the direction of the Poynting vector and the direction of the plane-wave propagation vector and is given by

$$\cos^2\rho = \frac{[1 + (\epsilon_3/\epsilon_1)\tan^2\phi]^2}{[1 + (\epsilon_3/\epsilon_1)^2\tan^2\phi](1 + \tan^2\phi)} . \qquad \text{(C1)}$$

For an extraordinary ray,

$$\epsilon(\omega_3) = \frac{\epsilon_1^2 + \epsilon_3^2\tan^2\phi}{\epsilon_1 + \epsilon_3\tan^2\phi} . \qquad \text{(C2)}$$

Combining Eqs. (C1) and (C2),

$$\epsilon(\omega_3)\cos^2\rho = \frac{\epsilon_1 + \epsilon_3\tan^2\phi}{1 + \tan^2\phi} . \qquad \text{(C3)}$$

For the geometry of Fig. 2(a), $\phi = 90°$, $\cos^2\rho = 1$, and $\epsilon(\omega_3) = \epsilon_3$. In Fig. 2(e), $\phi = 0°$, $\cos^2\rho = 1$, and $\epsilon(\omega_3) = \epsilon_1$. In Fig. 2(c), $\phi = 45°$ and $\epsilon(\omega_3) = \frac{1}{2}(\epsilon_1 + \epsilon_3)$.

In the case of a near cubic crystal oriented so that the [111] direction lies along the waveguide field, $\phi \approx 35.3°$, $\tan^2\phi = \frac{1}{2}$, and

$$\cos^2\phi = \frac{(2\epsilon_1 + \epsilon_3)^2}{3(2\epsilon_1^2 + \epsilon_3^2)} . \qquad \text{(C4)}$$

This expression was given for the special case treated in footnote f, Table I of Ref. 1.

Note that for the geometries of Figs. 2(b) and (d), the waveguide field is polarized as an *ordinary* wave, and $\epsilon(\omega_3) = \epsilon_1$.


[1]G. D. Boyd, T. J. Bridges, M. A. Pollack, and E. H. Turner, Phys. Rev. Lett. **26**, 387 (1971); T. J. Bridges, G. D. Boyd, and M. A. Pollack, in *Proceedings of the Symposium on Submillimeter Waves* (Polytechnic, Brooklyn, New York, 1971), Vol. 20.

[2]G. D. Boyd and D. A. Kleinman, J. Appl. Phys. **39**, 3597 (1968).

[3]R. W. Minck, R. W. Terhune, and C. C. Wang, Proc. IEEE **54**, 1357 (1966).

[4]G. D. Boyd, J. H. McFee, and H. Kasper, IEEE J. Quantum Electron. **7**, 563 (1971), see Appendix I for mks units.

[5]See Appendix 2 of Ref. 2; D. F. Nelson and M. Lax, Phys. Rev. B 3, 2795 (1971).

[6]M. A. Pollack and E. H. Turner, Phys. Rev. B **4**, 4578 (1971).

[7]E. P. Volkova and E. G. Yashchin, in *Proceedings of the Second All-Union Symposium on Nonlinear Optics, Novosibirsk, 1966* (Izd. AN SSSR, Novosibirsk, 1968).

[8]V. I. Tal'yanskii, A. A. Filimonov, and E. G. Yashchin, Fiz. Tverd. Tela **12**, 2756 (1970) [Sov. Phys.-Solid State **12**, 2224 (1971)].

[9]I. V. Ivanov and N. A. Morozov, Fiz. Tverd. Tela **8**, 3218 (1966) [Sov. Phys.-Solid State **8**, 2575 (1967)]; J. Phys. Soc. Jap. Suppl. **28**, 53 (1970).

[10]J. E. Geusic, S. K. Kurtz, T. J. Nelson, and S. H. Wemple, Appl. Phys. Lett. **2**, 185 (1963).

[11]C. Wuensche, Z. Angew. Phys. **19**, 501 (1965).

[12]R. C. Miller, Appl. Phys. Lett. **5**, 17 (1964).

[13]C. G. B. Garrett and F. N. H. Robinson, IEEE J. Quantum Electron. **2**, 328 (1966).

[14]G. M. Genkin, V. M. Fain, and E. J. Yashchin, Zh. Eksp. Teor. Fiz. **52**, 897 (1967) [Sov. Phys.-JETP **25**, 592 (1967)].

[15]C. G. B. Garrett, IEEE J. Quantum Electron. **4**, 70 (1968). The right-hand side of Eq. (60) must be multiplied by $[2/\mu\omega_i^2]$, as pointed out by Soref (Ref. 34).

[16]M. Lax and D. F. Nelson, Phys. Rev. B **4**, 3694 (1971).

[17]C. Flytzanis, Phys. Rev. B **6**, 1264 (1972).

[18]D. A. Kleinman, Phys. Rev. **126**, 1977 (1962).

[19]D. P. Akitt, C. J. Johnson, and P. D. Coleman, IEEE J. Quantum Electron. **6**, 496 (1970). Note that the expression relating $r_{41}$ to susceptibility [below Eq. (7) of this reference] should read $r_{41} = 2\chi^{(2)}(\omega;\omega;0)n^4$, and that the reduction of the data is therefore incorrect.

[20]A typographical error exists in the equivalent expression given in Ref. 1, Eq. (2), where $d_{eff}$ should be replaced by $(d_{eff})^2$.

[21]I. P. Kaminow and E. H. Turner, Proc. IEEE **54**, 1374 (1966).

[22]R. T. Smith and F. S. Welsh, J. Appl. Phys. **42**, 2219 (1971).

[23]R. Bechmann and S. K. Kurtz, in *Zahlenwerte und Funktionen aus Naturwissenschaften und Technik. Gruppe III: Kristall und Festkörperphysik*, edited by K.-H. Hellwege (Springer, Berlin, 1969), Vol. 2, p. 167.

[24]E. H. Turner (private communication) (unpublished measurements); and I. P. Kaminow and E. H. Turner, in *Handbook of Lasers with Selected Data on Optical Technology*, edited by R. J. Pressley (Chemical Rubber Company, Cleveland, 1971), p. 477.

[25]J. Jerphagnon, Phys. Rev. B **2**, 1091 (1970).

[26]G. D. Boyd, W. L. Bond, and H. L. Carter, J. Appl. Phys. **38**, 1941 (1967).

[27]W. L. Bond, J. Appl. Phys. **36**, 1674 (1965).

[28]A. S. Barker, Jr. and R. Loudon, Phys. Rev. **158**, 433 (1967).

[29]A. S. Barker, A. A. Ballman, and J. A. Ditzenberger, Phys. Rev. B **2**, 4233 (1970).

[30]W. D. Johnston, Phys. Rev. B **1**, 3494 (1970).

[31]A. S. Barker, Jr. and R. Loudon, Rev. Mod. Phys. **44**, 18

(1972).
[32]W. L. Faust, C. H. Henry, and R. H. Eick, Phys. Rev. **173**, 781 (1968).
[33]R. A. Cowley, Proc. R. Soc. A **268**, 109 (1962); Proc. R. Soc. A **268**, 121 (1962).
[34]R. A. Soref, IEEE J. Quantum Electron. **5**, 126 (1969).
[35]A. M. Glass and D. H. Auston, Opt. Commun. **5**, 126 (1969). (1972).
[36]A. M. Glass, Phys. Rev. **172**, 564 (1968).
[37]D. A. Kleinman, Phys. Rev. **118**, 118 (1960).
[38]C. Kittel, *Introduction to Solid State Physics*, 3rd ed. (Wiley, New York, 1966), p. 184. A relation between the thermal expansion coefficient and the anharmonicity of the lattice is given.
[39]T. G. Giallorenzi and C. L. Tang, Phys. Rev. **184**, 353 (1969).
[40]D. N. Klyshko, A. N. Penin, and B. F. Polkovnikov, Zh. Eksp. Teor. Fiz. Pis'ma Red. **11**, 11 (1970) [JETP Lett. **11**, 5 (1970)].
[41]D. P. Krindach and L. M. Krol, Opt. Spektrosk. **30**, 142 (1971) [Opt. Spectrosc. **30**, 73 (1971)].

PHYSICAL REVIEW B VOLUME 7, NUMBER 12 15 JUNE 1973

# Formulation to Include Phonon Effects in the Lattice-Statics Analysis of Electronic Defects and Polarons in Ionic Crystals*

John M. Vail
*Department of Physics, University of Manitoba, Winnipeg, Manitoba, R3T 2N2, Canada*
(Received 7 August 1972)

The Hamiltonian is derived for a dynamical crystal lattice of discrete ions with given ion-ion interaction, containing an excess-electron defect with nonharmonic lattice distortion. The electron-phonon part of the Hamiltonian turns out to include both linear and quadratic terms in the phonon variables. The contribution of the phonons to the energy of a defect such as an $F$ center in its ground state is derived in terms of a variational electronic wave function, using simple perturbation theory, to illustrate how this contribution can be incorporated in the lattice-statics analysis of such a defect. The large- and small-polaron Hamiltonians arising in the model are also presented and briefly discussed.

## I. INTRODUCTION

The method of lattice statics[1,2] provides a rigorous and practical method of evaluating the energy of a lattice defect in a crystal when the lattice distortion field is harmonic and the dynamical matrix of the perfect lattice is known. The method can be extended to include defects that involve nonharmonic lattice distortion,[3] provided that the interatomic forces are known, and to deal variationally with excess-electron defects.[3,4] As the name lattice statics implies, the method ignores dynamical lattice effects. However, these effects need to be considered, because they invariably contribute a defect-dependent zero-point energy and in the case of an excess-electron defect, they introduce phonon renormalization and electron self-energy, and determine the extent to which the electron-lattice interaction is nonadiabatic.

An outstanding example of a defect problem where progress has been seriously inhibited by inadequate treatment of phonon effects is the relaxed excited state (RES) of the $F$ center in NaCl-type alkali halides. It is known[5,6] that the electronic state of the RES in KCl is a parity mixture induced by interaction with the longitudinal-optical phonons. It has been conjectured for a long time[7] that the RES is somewhat delocalized, but this has not yet been settled experimentally in the case of KCl. For the case of KI, the RES has been experimentally found to be delocalized, but not a parity mixture.[8] Theoretically, the static-lattice model has so far failed to give a delocalized RES,[4,9] but the analysis by Wong and by Wang *et al.*,[6] which includes phonon effects in a continuum model of the lattice, does give some delocalization. Because this system is complicated, and apparently involves a delicate balance among the various factors contributing to the energy, the full theoretical analysis of both the parity-mixing mechanism and the delocalization property of the RES of the $F$ center should be approached through a model in which the electrical, elastic, and dynamical properties of the lattice are incorporated in a unified way. The object of the present work is to provide a formulation within which such an analysis can be performed, and to emphasize that presently available techniques render feasible the analysis of a wide range of phonon-dependent phenomena for a great variety of electronic defects in ionic crystals.

Such analyses are of practical, as well as fundamental, importance. For example, in the areas of applied photochromics[10] and thermoluminescence,[11] accurate characterization of the defect centers involved is a major outstanding problem area. Lidiard[12] has emphasized the feasibility and potential value of detailed defect calculations in "advancing the interpretation of experiments," and